We are IntechOpen, the world's leading publisher of Open Access books Built by scientists, for scientists

4,800
Open access books available

122,000
International authors and editors

135M
Downloads

Our authors are among the

154
Countries delivered to

TOP 1%
most cited scientists

12.2%
Contributors from top 500 universities

CLARIVATE ANALYTICS

BOOK CITATION INDEX

INDEXED

WEB OF SCIENCE™

Selection of our books indexed in the Book Citation Index
in Web of Science™ Core Collection (BKCI)

Interested in publishing with us?
Contact book.department@intechopen.com

Numbers displayed above are based on latest data collected.
For more information visit www.intechopen.com

A Dynamic Performance Model for Hybrid Wind/Gas Power Plants

Elias Tsoutsanis

Abstract

The scope of this chapter is to assess the performance of hybrid power plants and more specifically demonstrate the challenges of partnering the wind turbines with gas turbines. A dynamic engine model of a gas turbine along with a wind turbine model is developed to simulate plethora of scenarios for optimizing their operation in terms of efficiency, fuel consumption and NOx emissions. Moreover, a comparison between the hybrid power plant and a twin gas turbine power plant is carried out to assess the improvement in both NOx emissions and fuel consumption. The results demonstrate and illustrate the significant impact that dynamic performance modeling has in the optimization and controller design of hybrid power plant.

Keywords: wind energy, gas turbine, wind turbine, dynamic modeling, MATLAB/Simulink, engine control

1. Introduction

The expansion of wind power plants has transformed the gas turbines operation. The intermittent nature of wind prompts the gas turbines to operate with increased flexibility, for supporting their renewable plant partners and maintaining the stability of the electricity grid [1, 2]. Fast starts, shut downs and part load operation [3–5] are governing the operating profile of modern engines. It is vital, for an effective operation and maintenance (O&M) strategy, to employ tools and technologies that will support our understanding for these complex and nonlinear machines. Towards this end, gas turbine manufacturers have developed a suite of programs and systems that can model, monitor and analyse a plants performance [6].

Performance models of gas turbines, also called digital twins, play a significant role [7, 8] towards optimizing their operation. Apart from a few examples in the literature [9–11] most studies focus on steady state performance of gas turbines. Recently, their transient behaviour has attracted attention since they are required to act in partnership with renewables which are characterized by their intermittent nature.

Dynamic performance models of gas turbines are capable of facilitating the design of controllers that will enable the engines to fulfil their demanding new role

[12]. From a condition based maintenance point of view, dynamic engine models enable health monitoring, diagnostics [13–16] and prognostics [17, 18] capabilities.

Consequently, the recent shift in the operating envelope of the gas turbine has amplified the interest for developing real-time computationally efficient and accurate engine models that can help gas turbine operators to have an informed judgment about their assets. Furthermore, the monitored behaviour of the engine at transient conditions can facilitate the controller design for plethora of scenarios that involve gas turbines working in partnership with other energy sources.

Among the various methods [19–22] proposed in the literature for gas turbine performance simulation, the most common is the zero dimensional (0-D) approach [14, 23] which can be also used for real time monitoring, diagnosis and prognosis. From the transient performance analysis of a gas turbine one can identify important trends in performance that could potentially initiate surge of compressor or exceed temperature limits of engine. The simulation of plethora of scenarios provides important insights of the engine's behaviour and this is evident in cases where carrying out an experiment is either not feasible or may be catastrophic for the engine [24].

The two fundamental approaches for dynamic engine simulation are the iterative constant mass flow (CMF) method [25–27] and the inter-component volume (ICV) method [28]. Both of these methods have been extensively used for performance simulation studies of gas turbines [29–35]. The ICV approach is based on the flow imbalances during transient operation, where the CMF approach relies on the iterative minimization of key thermodynamic parameters that are initially guessed.

In this chapter, a model of a two-shaft gas turbine is developed in MATLAB/Simulink environment and coupled with a wind turbine model in order to assess the behaviour of the hybrid power plant in dynamic operating conditions. The developed engine model combines the above two approaches, since the CMF iterative method [36, 37] used for steady state is subsequently integrated with the ICV method for transient performance simulation.

The dynamic engine model utilizes component characteristic maps and is coupled to the governing thermodynamic equations of the engine cycle. The simulated scenarios of the engine operating under transient conditions provided key findings that would be hazardous for an actual gas turbine. An engine controller has been developed for enabling smooth and safe engine operation. The engine model has been validated towards PROOSIS [14] gas turbine simulation software. Furthermore, the behaviour of model is examined when the engine is coupled to a wind farm in a hybrid arrangement.

A generic model of a wind turbine has been developed in Simulink and coupled with the gas turbine model. The energy demand and the wind speed are designed to vary with respect to time which forces the gas turbine to work under transient conditions. This scenario provides additional information on the dynamic behaviour of the gas turbine and can also serve as a guide in controller design for hybrid plants. Finally, the hybrid plant's performance is compared to a twin gas turbine only power plant for estimating the capability of the gas turbines to shut down and their NO_x emissions.

The remainder of this chapter is organized as follows. In Section 2, the methodology employed for the transient performance simulation along with the controller design are described. The results of the case studies are presented and discussed in Section 3, followed by the conclusions in Section 4.

2. Methodology

2.1 Gas turbine mathematical model

For this study, the industrial gas turbine developed by the author in MATLAB/ Simulink [14], is briefly discussed in this chapter. The main components of the gas turbine are the compressor, combustor, and turbine. The gas turbine's exhaust gases are driving a free power turbine which is coupled to an electricity generator, as seen from **Figure 1**.

Station '1' denotes ambient air pressure and temperature. The following notation is used throughout the chapter. Temperatures and pressures are denoted by T_i and P_i, respectively where subscript $i = 1, 2, 3, 4, 5$ represents the engine station.

2.1.1 Compressor

The performance of the compressor is represented by a characteristic map which presents the interrelationships between pressure ratio $\pi_c = P_2/P_1$, isentropic efficiency η_c, corrected mass flow $\dot{m}_1\sqrt{T_1}/P_1$, and corrected shaft rotational speed $N/\sqrt{T_1}$. Scaled maps from PROOSIS [14] simulation software have been used in this model.

Once the outputs of the map are determined, the temperature rise ΔT_{12} across the compressor is computed as follows:

$$\Delta T_{12} = \frac{T_1}{\eta_c}\left[\left(\frac{P_2}{P_1}\right)^{\frac{\gamma_a-1}{\gamma_a}} - 1\right] \tag{1}$$

The work required to drive the compressor is given by

$$W_c = \dot{m}_1 \cdot c_{p_a} \cdot \Delta T_{12} \tag{2}$$

where c_{p_a} denotes the specific heat of air.

2.1.2 Combustor

The energy balance equation is governing the performance of the combustor as follows:

$$\dot{m}_1 \cdot c_{p_a} \cdot T_2 + \dot{m}_f \cdot LHV = \dot{m}_3 \cdot c_{p_g} \cdot T_3 \tag{3}$$

where *LHV* represents the fuel's low heat value, and c_{p_g} is the specific heat of combustion products. The heat input *HI* of the system is expressed as follows:

$$HI = \dot{m}_f \cdot LHV \tag{4}$$

which is further implemented for estimating the cycle's thermal efficiency η_{th}.
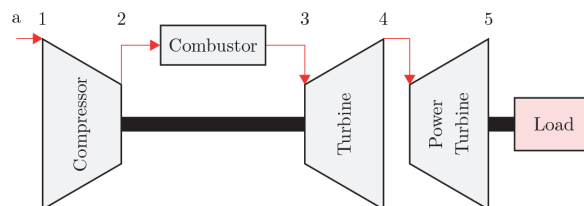

Figure 1.
Representation of the two-shaft engine model along with its station numbering [14].

Regarding emissions, the nitrogen oxides model developed by Rokke et al. [38], and validated by Pires et al. [39], is implemented in this gas turbine model. The NO_x emissions are estimated from the following equation:

$$NO_x = 18.1 \cdot (P_2/P_1)^{1.42} \cdot \dot{m}_1^{0.3} \cdot f^{0.72} \tag{5}$$

where P_2/P_1 denotes compressor pressure ratio, $\dot{m}_1$ denotes air mass flow rate, and f denotes fuel to air ratio (i.e. $\dot{m}_f/\dot{m}_1$). The NO_x emissions are measured in parts per million by volume (ppmv) at 15% O_2.

2.1.3 Turbine

Similar to the compressor, turbine performance is represented by a set of characteristic maps that present the interrelationships between turbine pressure ratio π_t, corrected mass flow $\dot{m}_3\sqrt{T_3}/P_3$, efficiency η_t, and corrected rotational speed $N/\sqrt{T_3}$.

It follows that the temperature drop ΔT_{34} across the turbine is computed by:

$$\Delta T_{34} = \eta_t \cdot T_3 \left[1 - \left(\frac{1}{\pi_t}\right)^{\frac{\gamma_g-1}{\gamma_g}}\right] \tag{6}$$

where γ_g is the heat capacity ratio of combustion products and for preliminary performance calculations it may be assumed constant, i.e. $\gamma_g = 1.33$. The work extracted by the turbine is given by:

$$W_t = \eta_m \cdot \dot{m}_3 \cdot c_{p_g} \cdot \Delta T_{34} \tag{7}$$

where c_{p_g} represents the specific heat of combustion gases and η_m is the mechanical efficiency.

2.1.4 Power turbine

Similar to the turbine, the performance of the power turbine is represented by characteristic maps that present the interrelationship between pressure ratio π_{pt}, corrected mass flow $\dot{m}_4\sqrt{T_4}/P_4$, efficiency η_{pt}, and corrected rotational speed $N_{pt}/\sqrt{T_4}$.

The temperature drop ΔT_{45} across the power turbine is given by:

$$\Delta T_{45} = \eta_{pt} \cdot T_4 \left[1 - \left(\frac{1}{\pi_{pt}}\right)^{\frac{\gamma_g-1}{\gamma_g}}\right] \tag{8}$$

In this chapter, the speed of the free power turbine is assumed constant since it is connected to an electricity generator. The work delivered by the power turbine is the useful work UW of the cycle and is given by:

$$UW = \dot{m}_4 \cdot c_{p_g} \cdot \Delta T_{45} \tag{9}$$
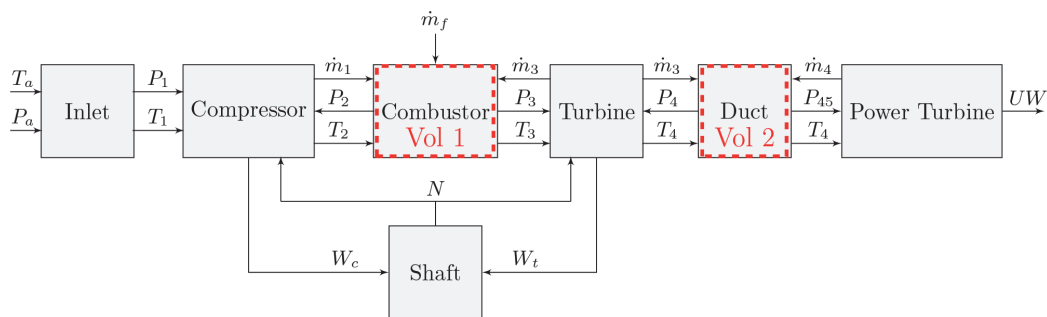
4

Figure 2.
Schematic representation of the modular computational interaction of the transient engine model [14].

The thermal efficiency of the gas turbine system is given by:

$$\eta_{th} = 100 \cdot \frac{UW}{HI} \qquad (10)$$

and expressed as a percentage.

2.2 Dynamic simulation

The ICV method has been implemented in the development of the engine model in MATLAB/Simulink environment [45, 46]. This method works on the principle that mass flow imbalances occur during transient operation. Two plenum volumes, one before the turbine and one after the turbine, have been added to the model, as seen from **Figure 2**. The component maps for compressor, turbine and power turbine are the same as the steady state model.

The fuel addition initiates the mass flow imbalances which are used to calculate the rate of pressure variations. The description of the process is provided in the following subsections.

2.2.1 Dynamics

Combustor: Volume 1—The mass flow continuity is used to calculate the pressure in the combustor volume, as follows:

$$\frac{dP_2}{dt} = \frac{RT_2}{V_1}\left(\dot{m}_1 + \dot{m}_f - \dot{m}_3\right) \qquad (11)$$

where R, V_1, and P_2 denote gas constant, combustor volume, and compressor delivery pressure, respectively. The combustor outlet pressure can be calculated as a simple proportionality from:

$$\frac{P_2 - P_3}{P_2} = PLF \qquad (12)$$

where PLF is the combustor pressure loss factor and for this study a 5% drop in pressure is assumed.

Duct: Volume 2—The pressure at the exit of the gas turbine is given by:

$$\frac{dP_4}{dt} = \frac{RT_4}{V_2}\left(\dot{m}_3 - \dot{m}_4\right) \qquad (13)$$

where V_2 and P_4 denote duct volume and turbine delivery pressure, respectively. The turbine outlet pressure can be calculated as a simple proportionality from:

$$\frac{P_4 - P_{45}}{P_{45}} = PLF \tag{14}$$

where *PLF* is the turbine pressure loss factor and for this study we assumed that there are no losses between the turbine and the power turbine, i.e. $P_4 = P_{45}$.

Shaft—The difference between compressor W_c and turbine work W_t, is used in the computation of the engine's acceleration which is given by:

$$\frac{dN}{dt} = \left(\frac{30}{\pi}\right)^2 \cdot \frac{W_t - W_c}{JN} \tag{15}$$

where J is the shaft polar moment of inertia measured in kg m^2.

System states—Assuming that the system's state is denoted by u, and the set of variables is represented by x then the state and control variables are defined as follows:

$$x = [P_2, P_4, N]^T \tag{16}$$

$$u = \dot{m}_f \tag{17}$$

The pressures P_2 and P_4, and shaft rotational speed N, at design point conditions are the input parameters of the model. To summarize, the gas turbine dynamics may be expressed as:

$$\frac{dx}{dt} = f(x, u) \tag{18}$$

2.2.2 Simulation process

The initial state values for the transient engine model are summarized in **Table 1**.

It is noted that at steady state conditions the derivatives dP_2/dt, dP_4/dt and dN/dt are all zero.

2.3 Controller design

Controller design is crucial for achieving a safe and reliable engine operation. Among a variety of controllers suitable for gas turbine engines, the one implemented in this study is a PI controller. Its objective is to regulate the fuel flow rate $\dot{m}_f$ by comparing the speed demand N_d with the measured speed N_m of the gas turbine. To achieve this both the fuel flow actuator and the speed sensor are modelled by simple first order transfer functions [23, 32].

The process of the controller's operation is schematically represented in **Figure 3**. The actuating signal ε is driving the controller to generate a demand for

Symbol	Parameter	Value	Units
P_{2_0}	Compressor discharge pressure	1472	kPa
P_{4_0}	Turbine exit pressure	406	kPa
N_0	Gas generator shaft rotational speed	9000	rpm

Table 1.
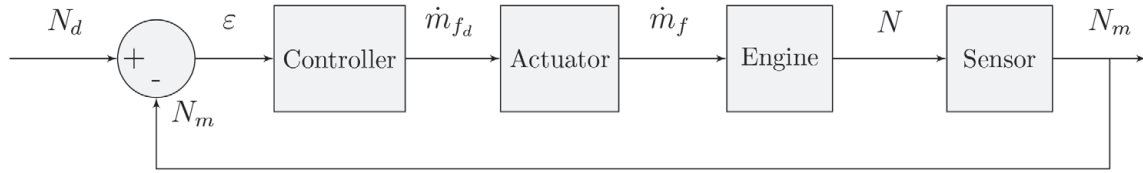*The initial state for the transient engine model.*

Figure 3.
Block diagram of a speed controller for fuel flow regulation.

fuel flow rate $\dot{m}_{f_d}$ which is then translated to the movement of the actuator in order to admit fuel $\dot{m}_f$ into the combustor. The engine responds to this command and the measured engine speed is compared to the desired one.

The control function of this PI controller can be expressed as follows:

$$\dot{m}_{f_d}(t) = K_p \varepsilon(t) + K_i \int_0^t \varepsilon(t) dt \tag{19}$$

where $\varepsilon(t) = N_d(t) - N_m(t)$, and K_p, K_i denote the coefficients of the proportional and the integral terms, respectively. The transfer functions for the fuel system actuator and the speed sensor are given by:

$$G_1(s) = \frac{\dot{m}_f(s)}{\dot{m}_{f_d}(s)} = \frac{1}{0.05s + 1} \tag{20}$$

$$G_2(s) = \frac{N_m(s)}{N(s)} = \frac{1}{0.05s + 1} \tag{21}$$

The reader is prompted to [32], if a more advanced controller design is pursued. However, for this study which focuses on enabling the engine to respond in a safe manner during transient operation the proposed controller is capable to achieve this objective. The proposed model has been validated towards PROOSIS gas turbine simulation software and a full description of the validation case studies can be found in [14].

2.4 Wind turbine model

A generic model of a wind turbine, available from MATLAB/Simulink [40], is used in this study in order to assess the operation of a hybrid power plant when the gas turbine is coupled to a wind farm.

The wind turbine's performance is governed by pitch angle β, wind speed V_{wind} and wind turbine speed N_{wt}. These are commonly represented in a performance map, as seen in **Figure 4**. The power output of the wind turbine UW_{wt} is given by [40]:

$$UW_{wt} = C_p \cdot \eta_{mech} \cdot \eta_{elect} \cdot \frac{1}{2} \cdot \overline{\rho} \cdot A \cdot \overline{V_{wind}^3} \tag{22}$$

where $\overline{\rho}$ denotes the mean air density over the rotor swept area A, η_{mech} denotes mechanical efficiency of bearings, gear box, generator, etc., η_{elect} denotes electrical efficiency of transformer, converter, etc., $\overline{V_{wind}^3}$ denotes the mean of the cubic wind speed and C_p denotes the power coefficient. The power coefficient C_p depends on the blade tip ratio λ and the blade pitch angle β. For this study a generic equation is used as follows [40]:

$$C_p(\lambda, \beta) = C_1(C_2/\lambda_i - C_3\beta - C_4)e^{\frac{-C_5}{\lambda_i}} + C_6\lambda \tag{23}$$

where $C_1 = 0.5176$, $C_2 = 116$, $C_3 = 0.4$, $C_4 = 5$, $C_5 = 21$, and $C_6 = 0.0068$. The blade tip ratio relationship with pitch angle is given by:

$$\frac{1}{\lambda_i} = \frac{1}{\lambda + 0.08\beta} - \frac{0.035}{\beta^3 + 1} \tag{24}$$

The wind turbine model has three inputs namely β, V_{wind}, N_{wt}, and one output UW_{wt}.

The hybrid gas/wind power plant consists of a gas turbine and a wind farm with variable power output. The total power output UW_{total} from the hybrid power plant is given by:

$$UW_{total} = UW_{gt} + UW_{wt} \tag{25}$$

The energy gap ΔW imposed by the wind turbines is covered by the gas turbine. This difference is expressed as follows:

$$\Delta W = DW - UW_{total} \tag{26}$$

Any instant that the demand is not met, then the gas turbine has to respond by adjusting its fuel flow regulation. An algebraic constraint is used to constrain the difference to zero (i.e. $\Delta W = 0$) by tuning the value of the demanded speed from the gas turbine. The schematic diagram of the developed models is shown in **Figure 5**.

It should be highlighted that the wind turbine used here is a generic and simple model that fits the objective of this study. If one seeks a high fidelity performance assessment of wind turbines, the reader is prompted to studies [41–44] which address the dynamic response of the wind turbine at a greater detail.
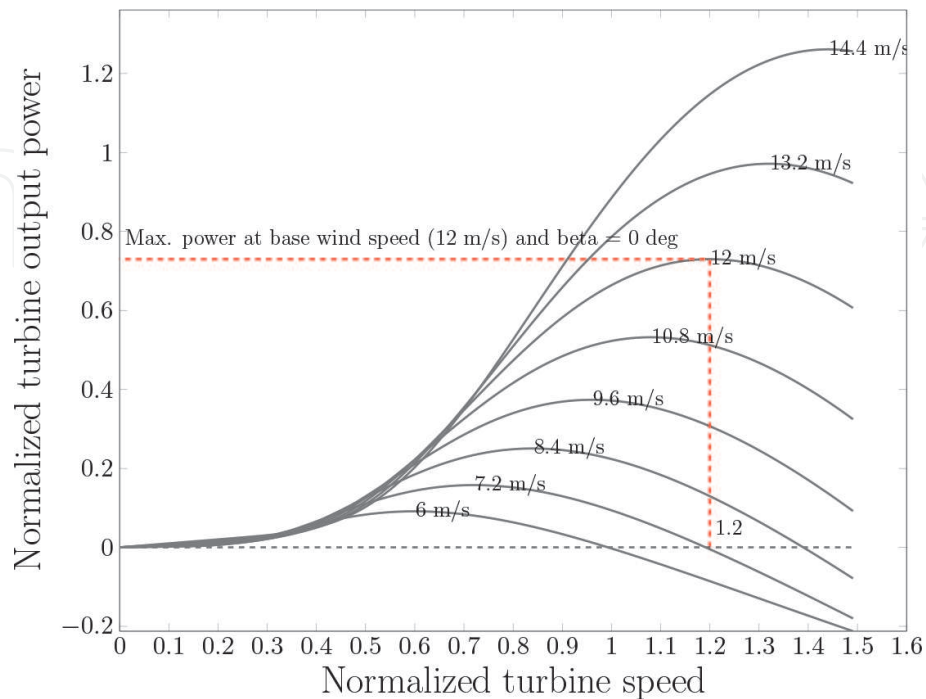

Figure 4.
Wind turbine performance map representing the power output as a function of generator speed, for different wind speeds and for a blade pitch angle β = 0 degrees [14].
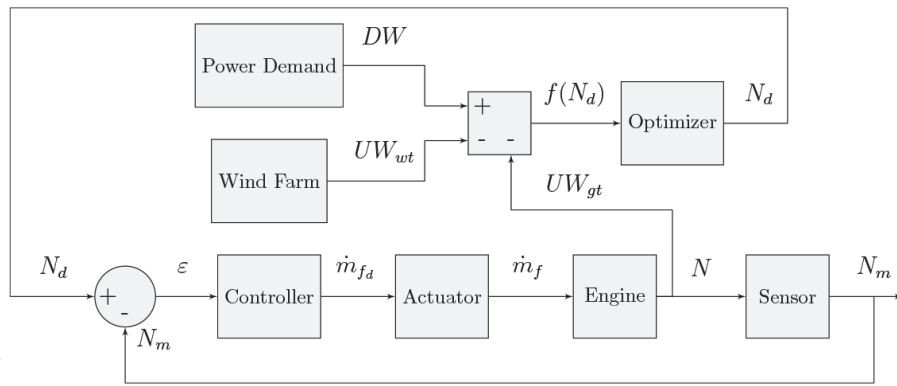
Figure 5.
Block diagram of the hybrid gas/wind controller and optimization module [14].

3. Results and discussions

3.1 Case study 1: transient step response with PI controller

This case study examines the transient performance of the engine when a PI controller is implemented. The controller enables a smooth and safe engine operation. The schematic diagram of this control arrangement is shown in **Figure 6**.

The PI controller tunes the fuel flow rate according to the actuating signal arising from the difference of demanded N_d and measured N_m shaft speed. The controller design toolbox in Simulink provides a visual representation of the system's behaviour and the user can select the desired response characteristics. this translates into a unique set of control coefficients K_p and K_i, that update the engine's controller. The compressor surge and combustor flame-out limits, described in detail in [14], are also integrated into the controller subsystems of the model, as seen from **Figure 7**.

The controller has to regulate the fuel flow into the engine by ensuring that this command lies within the surge and flame-out limits. So depending on the demanded shaft speed N_d and the ambient conditions T_1, P_1, two look up tables are used to calculate the fuel flow rates that correspond to the surge $\dot{m}_{f_{max}}$ and flame-out $\dot{m}_{f_{low}}$ limits of the engine. When then fuel flow rate computed by the PI controller violates these limits, then a switch is used to bound the final fuel flow rate demand $\dot{m}_{f_d}$ within them, as seen from **Figure 7**.

For this case study, the coefficients of the PI controller and the transient response characteristics are summarized in **Table 2**.

Repeating the simulation of the engine model in Simulink results in a controlled engine behaviour. A comparison between the behaviour of the engine model without and with a PI controller is seen in **Figure 8**.

It becomes clear from **Figure 8** that T_3 is no longer exhibiting an oscillating behaviour during this sudden increase in the demanded engine speed, since the fuel flow has been modified through the PI controller.
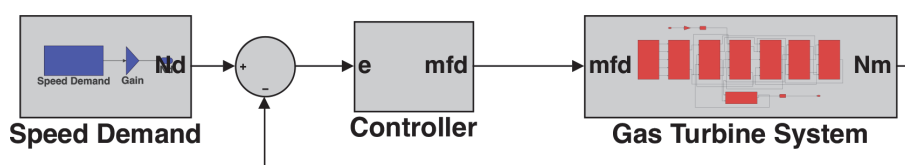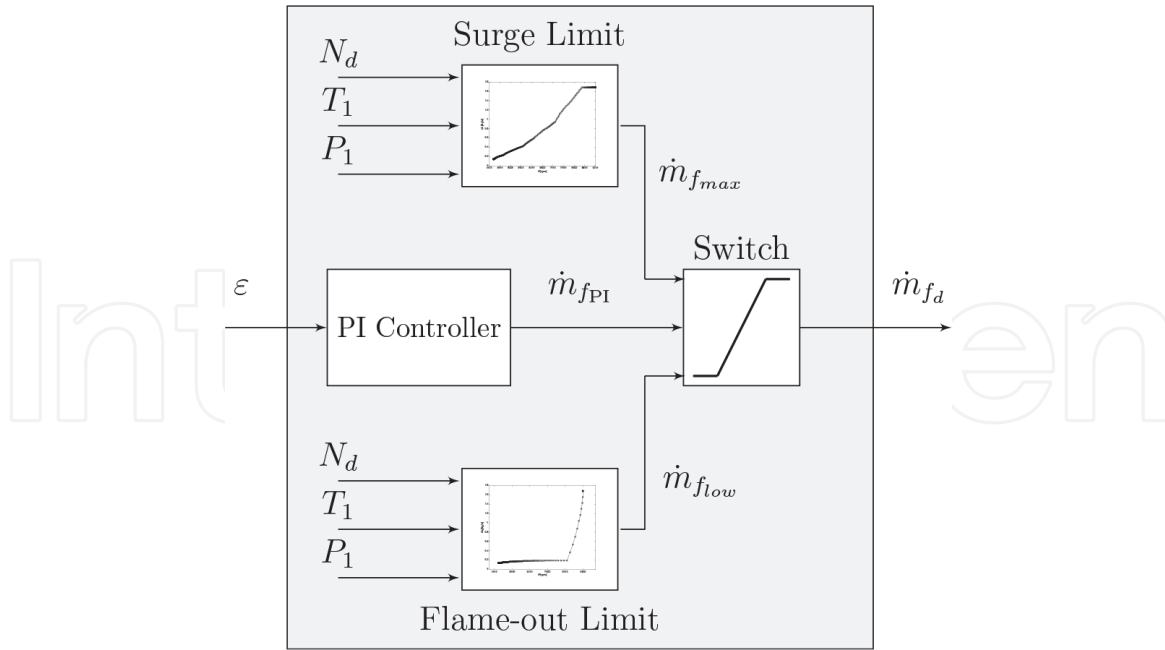

Figure 6.
Schematic layout of the MATLAB/Simulink model with the controller [14].

Figure 7.
Detailed block diagram of the controller subsystem with the surge and flame-out limiting functions implemented as look-up tables [14].

Parameter	Value	Units
K_p	8.562E−05	—
K_i	0.794E−03	—
Rise time	0.896	Seconds
Settling time	1.676	Seconds
Overshoot	0	%
Peak	1	—

Table 2.
The parameters of the PI controller [14].

It is evident from **Figure 8** that without a PI controller, where the fuel flow command was not regulated, a large operational regime has occurred that would have violated the firing temperature limits and may have led to compressor surge. The implemented controller has resolved the above issue by regulating a fuel flow rate that results in a smoother engine operating profile.

3.2 Case study 2: hybrid gas/wind power plant

The objective of this case study is to assess the performance of the gas turbine when it is coupled to a wind farm. The design point performance of the wind turbine is summarized in **Table 3**, and this refers to a generic wind turbine model available in [40].

The time increment of the simulation is 1 ms and for a 10 s simulation there are 10,000 operating points. The results are correlated to a 10 h operation, which means that for every minute there are 16 operating points. The size of the data support the above decision as the nonlinear behaviour of the gas turbine is well captured. The hybrid power plant, seen in **Figure 9**, consists of a gas turbine and 14 wind turbines.
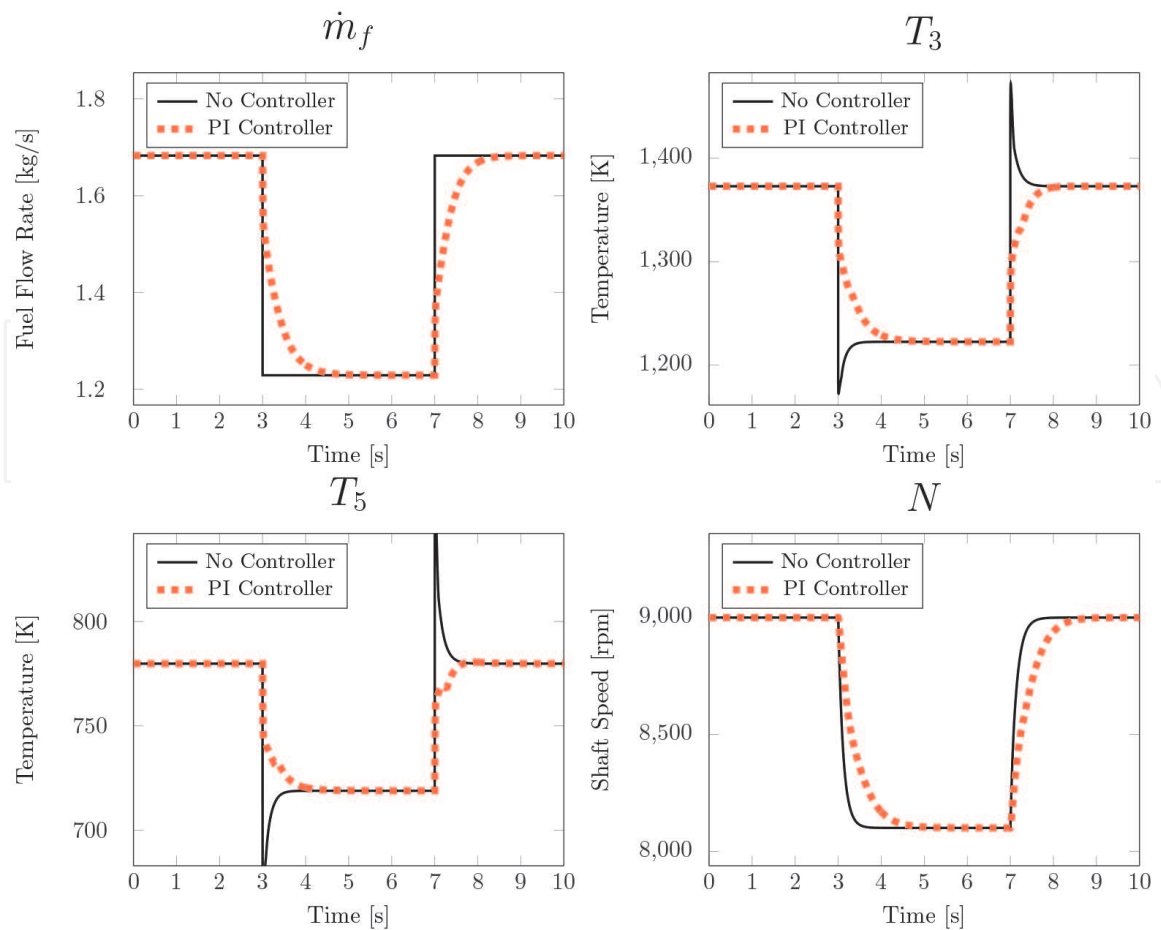
Figure 8.
Variation of the simulated measurements with respect to time from MATLAB/Simulink model of case study 1.

Symbol	Parameter	Value	Units
V_{wind}	Wind speed	12	m/s
N_{wt}	Generator speed	1800	rpm
UW_{wt}	Power output	1500	kW

Table 3.
The design-point performance specifications of the wind turbine [14].

The variation of wind speed with respect to time can be seen from **Figure 10**. This variation is designed by having in mind that the gas turbine will commence its operation close to its design point. At the 2 and 5 h mark the gas turbine will have to respond to this change by decelerating and following the demand according to the intermittent power output of the wind turbines.

The required power from the power plant ranges from 28 MW up to 37 MW. The above is combined with the varying wind speed, and the resultant power output of each system is shown in **Figure 11**.

The PI controller discussed in case study 1 is utilized here in combination with the algebraic constraint optimizer. The PI controller parameters are the same as case study 1.

The power output varies with respect to time, as seen from **Figure 12**, where the percentage of power output of each system is illustrated. The wind farm contributes up to 70% of the demanded power, while the maximum power output contribution from the gas turbine is 75%. A closer look at the shaft rotational speed N and exhaust gas temperature T_5, from **Figures 13** and **14**, reveals the dynamic response of the gas turbine.
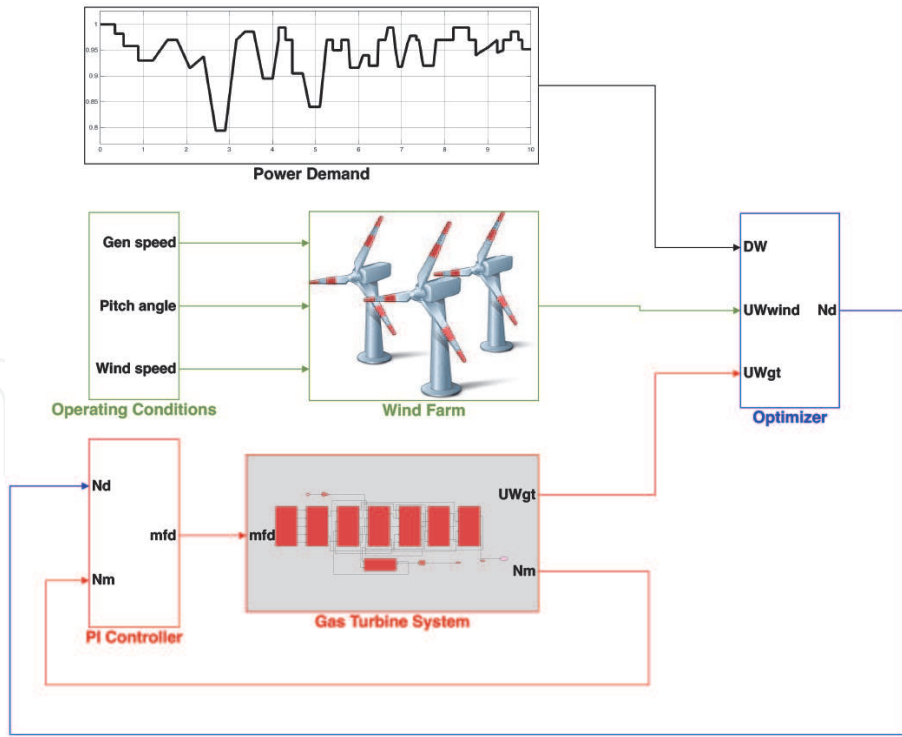
Figure 9.
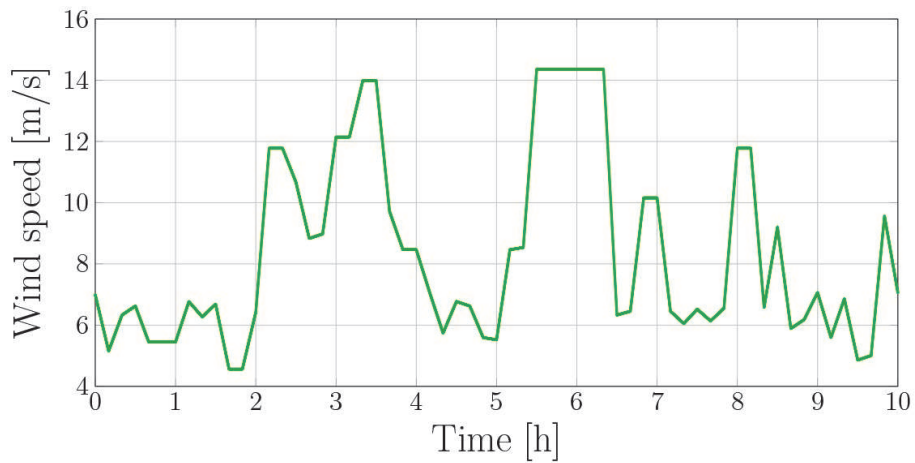*Schematic layout of the hybrid gas/wind power plant in Simulink [14].*

Figure 10.
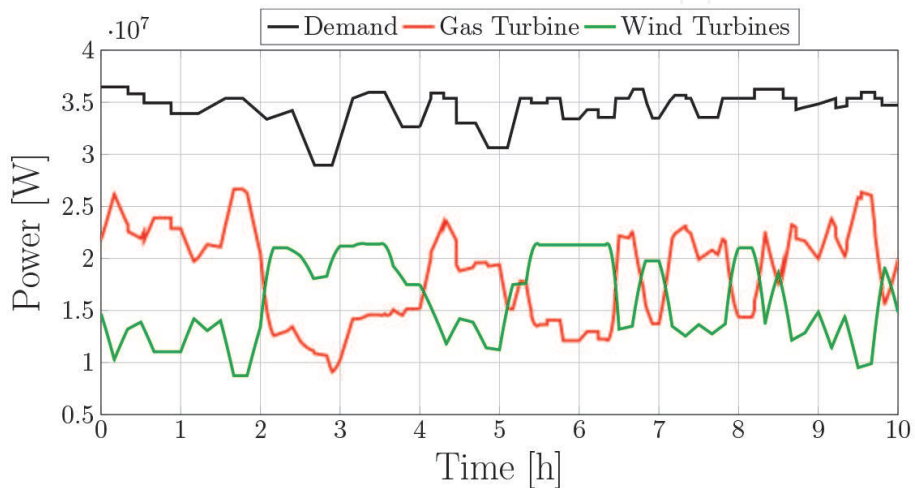*Variation of wind speed with respect to time [14].*

Figure 11.
Time response of the gas turbine and the wind turbines to meet the fluctuating demand [14].
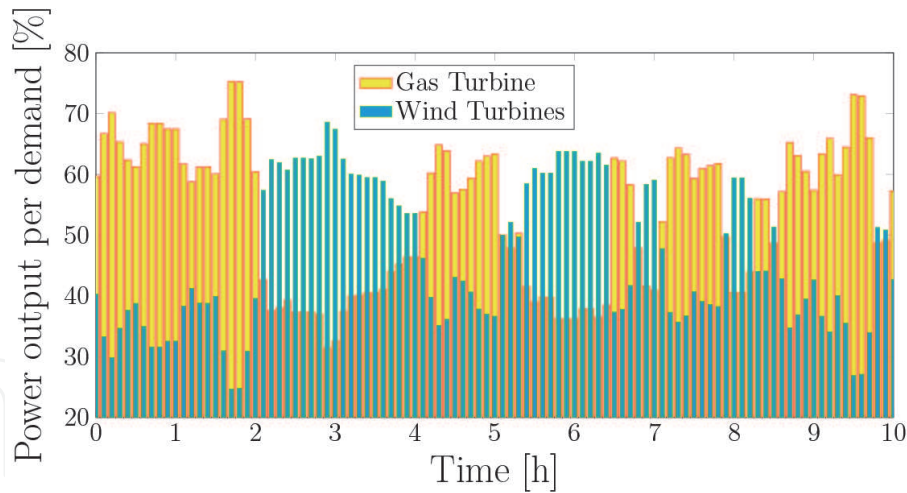
12

Figure 12.
The variation of the power output from the gas and wind turbines expressed as a percentage to total power demand with respect to time [14].
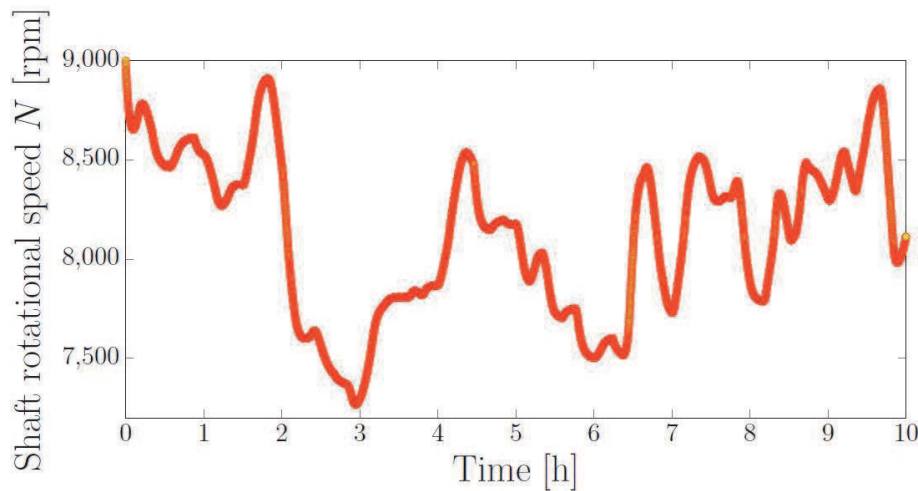

Figure 13.
The variation of the gas turbine shaft rotational speed with respect to time [14].

Figure 13 shows that the speed of the gas turbine's is dependent on the wind speed which essentially dominates the behaviour of the wind farm. A pattern of similar form is shown in the variation of the gas turbine's exhaust temperature, seen in **Figure 14**.

3.3 Case study 3: hybrid power plant comparison with a twin gas turbine plant

The primary aim of this case study is to carry out a comparative study between the hybrid power plant and a plant that consists of two gas turbines only. To make the comparison easier the hybrid power plant is referred to as Plant A and the twin gas turbine plant is referred to as Plant B. Plant B's gas turbine engines are identical to the one of Plant A. The demanded power from both plants is the same. The simulated scenario of this study corresponds to 10 h operation. The NO_x emission and fuel consumption for both plants are assessed. The power demanded from each plant can be seen in **Figure 15**.

It should be noted that the demanded power signal has been designed in such a way so that there are two occasions during which the power drops significantly and peaks up again. There are two periods for which the engine of Plant A will be required to shut down, in order to assess its shut down capabilities.
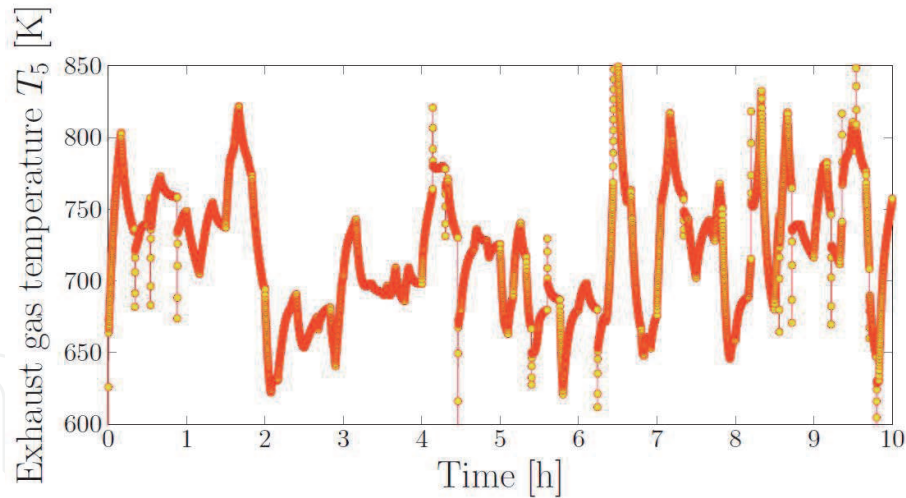
Figure 14.
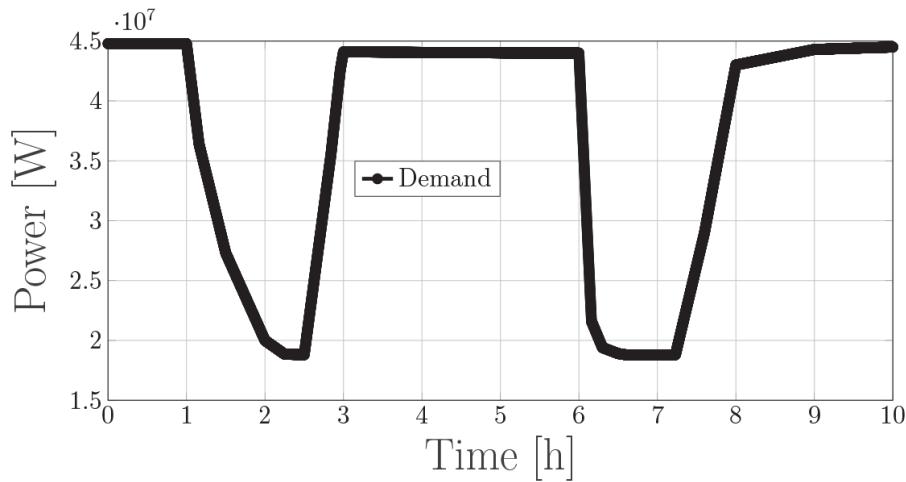*The variation of the gas turbine exhaust temperature with respect to time [14].*

Figure 15.
Representation of power demanded from Plants A and B with respect to time [14].

Figure 16 shows that the power output from the gas turbine and wind turbines of Plant A. One hour into the operation, the gas turbine slowly decreases its power output until the 2 h mark and will remain shut for half hour. After the 30 min break the engine will fire up again, reach a power output of 25 MW and hover over this power setting for another 3 h. At the 6 h mark, the engine will experience another shut down event and will remain inactive for 1 h before starting up again and remaining at approximately 26 MW for the final 2 h of operation.

1 h of operation, the power required from the engine decreases slowly with respect to time and forces the engine to shut down and remain inactive for 30 min. It then starts up again and in approximately 25 min reaches a power setting close to its design point for the next 3 h. At the 6 h mark, the power output reduces faster as it takes approximately 10 min to shut down the engine.

Traditionally, current industrial gas turbine engines are capable of shutting down in less than 10 min [47]. On the other hand, a hot start up (i.e. less than 8 h standstill) process may take less than 0.1 h (i.e. 6 min) with a ramp rate up to 15% of nominal load per minute [48]. In addition, the fastest the start-up [49] and shut downs are, the greater the economic benefit and the life cycle reduction are going to be. Therefore start up and shut down processes should be optimized by taking into consideration several operational constraints. The gas turbine of the hybrid plant in
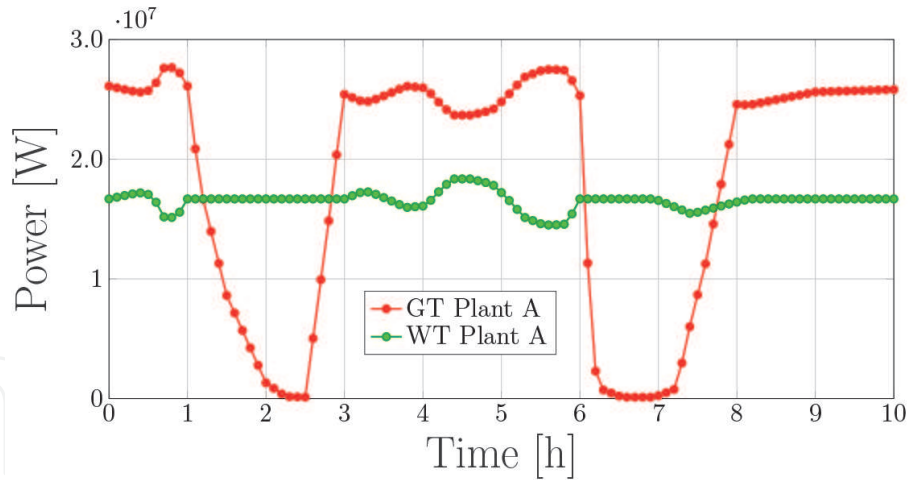
Figure 16.
The variation of the power output from the gas and wind turbines of Plant A expressed with respect to time [14].
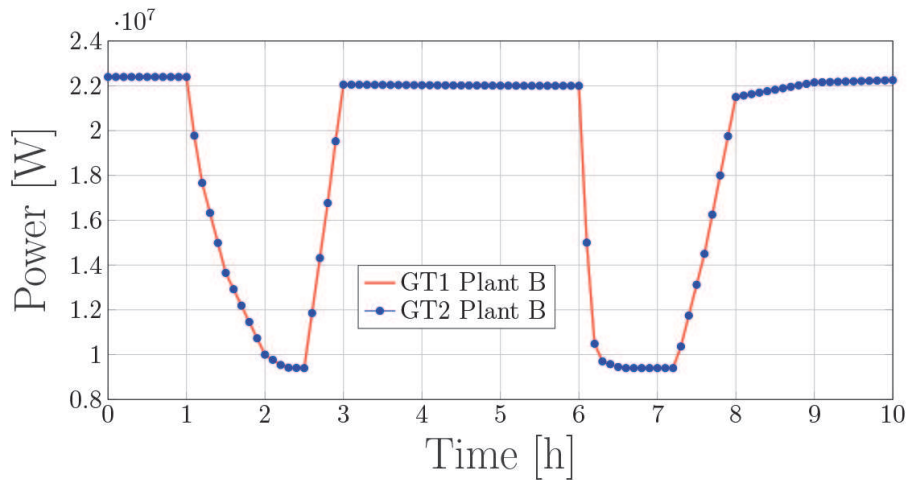

Figure 17.
The variation of the power output from the gas turbines of Plant B expressed with respect to time [14].

this case study is exhibiting fast response behaviour which is beneficial for the wind turbines (**Figure 17**).

Meanwhile, the wind turbines remain operational during the entire 10 h. Given that the power demanded from the plant has two occasions with significant load fluctuations, both of them have to be accommodated by the flexibility of the gas turbine since the wind farm's power capacity has a priority in the grid for this hybrid power plant.

For Plant B, both gas turbines have an identical load distribution, as shown in **Figure 17**, and meet the demanded power. In contrast to the Plant A gas turbine, Plant B engines operate at part load off-design conditions. The power output has a substantial effect in the NO_x emissions of gas turbines, as observed from Eq. (5), since the higher the pressure ratio, the higher the TET and therefore the higher the emissions are going to be.

The NO_x emissions of both plants are shown in **Figure 18**. As expected, the NO_x emissions from Plant B are significantly higher than those of Plant A. The amount of NO_x emissions reduction is illustrated in **Figure 19**, where the emissions of Plant A are compared to those of Plant B as a percentage.

The NO_x emissions of Plant A are initially 43% less than that of Plant B and increase to 100% when the gas turbine of Plant A shuts down. Regarding the fuel consumption, Plant A consumes less fuel compared to Plant B, and this accounts to
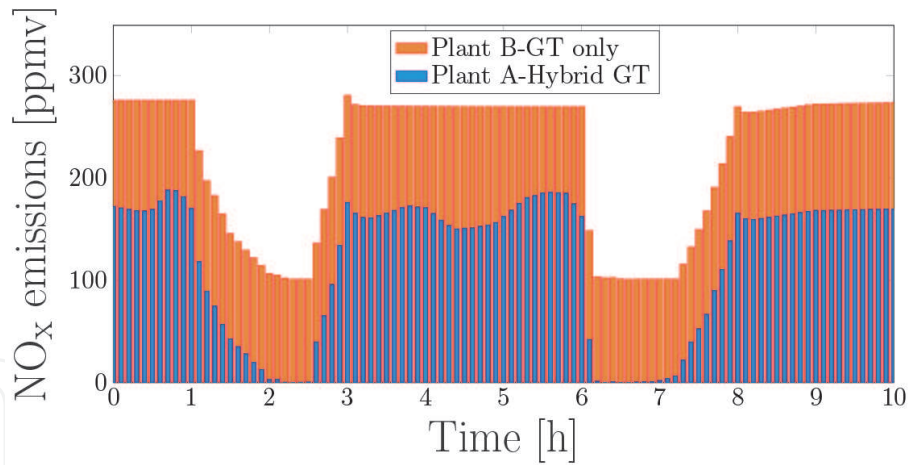
Figure 18.
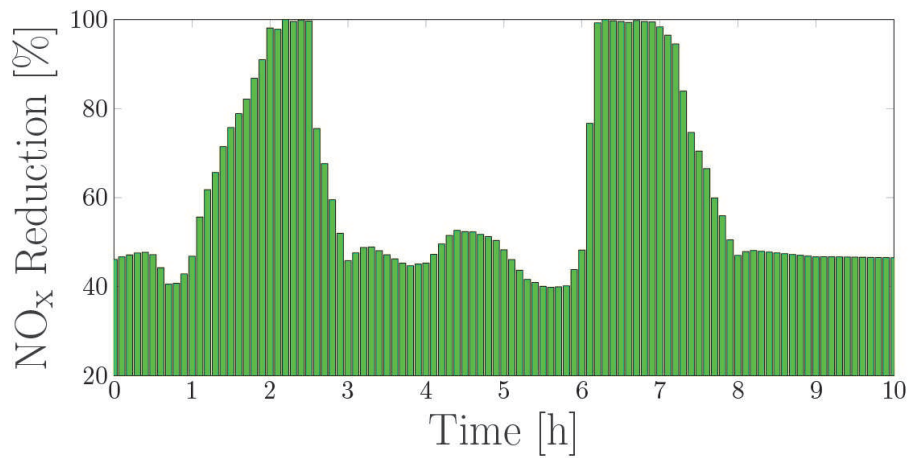*The variation of NO$_x$ emissions for Plants A and B with respect to time [14].*

Figure 19.
The variation of NO$_x$ emissions percentage reduction of Plant A in comparison to Plant B with respect to time.
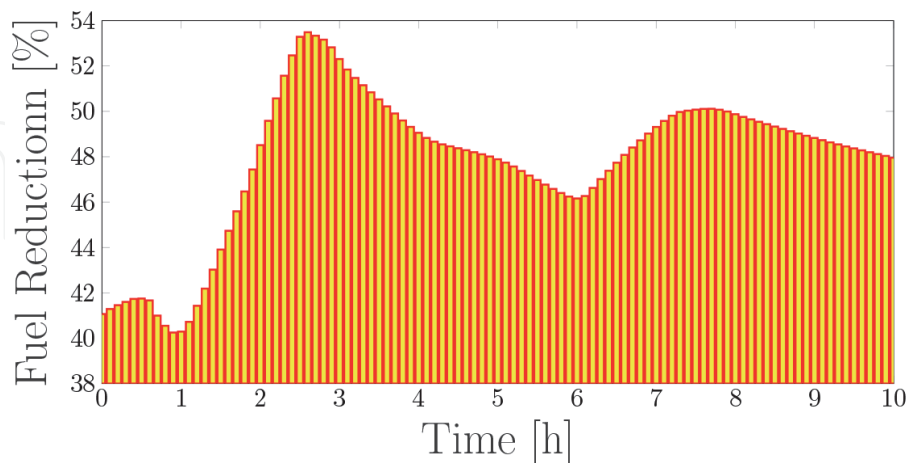

Figure 20.
The accumulated variation of fuel percentage reduction of Plant A in comparison to Plant B with respect to time [14].

48%, as seen in **Figure 20**. Note that the fuel reduction represented in **Figure 20** refers to the accumulated fuel flow. This case study amplifies the significance of transient observations arising from simulating various dynamic operating scenarios of gas turbines. Key findings about their behaviour, performance, environmental impact and flexibility add value to our understanding of this technology especially

when it is coupled with renewables. Finally, fast transient gas turbine manoeuvers are essential to the stability of the grid in hybrid power plant arrangements. Additional promising technologies for wind speed forecasting might enable smoother transient gas turbine operation in a hybrid gas/wind power plant.

As far as practical issues are concerned the developed model can be further improved by a number of useful additions such as variable pitch control of the wind turbine [50, 51], wind forecasting models [51], and adaptive model-tuning. Another important aspect of this developed model is the fact that it enables users to simulate numerous scenarios and can potentially feed its simulated measurements into a multi-objective optimization process for improving the performance of gas turbine. In addition, the model can accommodate degradation case studies [17] at component and system level for improving the prediction accuracy and the computational efficiency of diagnostic and prognostics algorithms.

4. Conclusions

In this chapter, a novel gas turbine engine model is presented that aims to capture the nonlinear behaviour of modern gas turbines. The gas turbine model is created in MATLAB/Simulink.

The engine model consolidates the iterative constant mass flow approach in steady state conditions for initializing the state parameters to the dynamic model, which utilizes the inter-component volume technique. The dynamic response of the model has been evaluated for a hybrid gas/wind power plant comprising of 14 wind turbines. The result of this analysis features the quick transient trajectories that the gas turbine encounters as the consequence of variable wind speeds and fluctuating energy demand. In addition, the behaviour of the hybrid power plant underlined the requirement for transient simulation scenarios since several operating challenges must be addressed to maintain stability in the grid. Finally, the comparative study of the hybrid power plant to a twin gas turbine plant for a 10 h operation showed that the NO_x emissions decrease from 40% to 100% depending on the power setting of the engine.

The modularity, robustness and computational efficiency are key feature of the developed engine model. The above features facilitate the performance assessment and controller design of gas turbines that operate under transient conditions. Furthermore, the developed engine model can improve our understanding for these complex machines and enables us to optimize the energy dispatch of a hybrid power plant. The proposed model can also serve as a useful tool and guide in optimizing the performance of a gas turbine powered-plant, monitoring its emissions and establishing a reference for subsequent model-based diagnostics and prognostics studies.

Author details

Elias Tsoutsanis
School of Engineering, University of Birmingham, Edgbaston, UK

*Address all correspondence to: e.tsoutsanis@bham.ac.uk

IntechOpen

References

[1] Barelli L, Bidini G, Ottaviano A. Integration of SOFC/GT hybrid systems in micro-grids. Energy. 2017;**118**:716-728

[2] di Gaeta A, Reale F, Chiariello F, Massoli P. A dynamic model of a 100 kW micro gas turbine fuelled with natural gas and hydrogen blends and its application in a hybrid energy grid. Energy. 2017;**129**:299-320

[3] Mehrpanahi A, Payganeh G, Arbabtafti M. Dynamic modeling of an industrial gas turbine in loading and unloading conditions using a gray box method. Energy. 2017;**120**:1012-1024

[4] Barelli L, Bidini G, Ottaviano A. Part load operation of a SOFC/GT hybrid system: Dynamic analysis. Applied Energy. 2013;**110**:173-189

[5] Bahlawan H, Morini M, Pinelli M, Spina PR, Venturini M. Development of reliable narx models of gas turbine cold, warm and hot start-up. Journal of Engineering for Gas Turbines and Power. 2017;**140**(7)

[6] Tahan M, Tsoutsanis E, Muhammad M, Abdul Karim ZA. Performance-based health monitoring, diagnostics and prognostics for condition-based maintenance of gas turbines: A review. Applied Energy. 2017;**198**:122-144

[7] Barsali S, De Marco A, Giglioli R, Ludovici G, Possenti A. Dynamic modelling of biomass power plant using micro gas turbine. Renewable Energy. 2015;**80**:806-818

[8] Ponce CV, Saez D, Bordons C, Nunez A. Dynamic simulator and model predictive control of an integrated solar combined cycle plant. Energy. 2016;**109**: 974-986

[9] Alobaid F, Mertens N, Starkloff R, Lanz T, Heinze C, Epple B. Progress in dynamic simulation of thermal power plants. Progress in Energy and Combustion Science. 2017;**59**:79-162

[10] Ablay G. A modeling and control approach to advanced nuclear power plants with gas turbines. Energy Conversion and Management. 2013;**76**: 899-909

[11] Kang S, Ahn K. Dynamic modeling of solid oxide fuel cell and engine hybrid system for distributed power generation. Applied Energy. 2017;**195**: 1086-1099

[12] Cao Y, Dai Y. Comparative analysis on off-design performance of a gas turbine and ORC combined cycle under different operation approaches. Energy Conversion and Management. 2017;**135**: 84-100

[13] Tsoutsanis E, Meskin N, Benammar M, Khorasani K. A component map tuning method for performance prediction and diagnostics of gas turbine compressors. Applied Energy. 2014;**135**:572-585

[14] Tsoutsanis E, Meskin N. Dynamic performance simulation and control of gas turbines used for hybrid gas/wind energy applications. Applied Thermal Engineering. 2019;**147**:122-142

[15] Amozegar M, Khorasani K. An ensemble of dynamic neural network identifiers for fault detection and isolation of gas turbine engines. Neural Networks. 2016;**76**: 106-121

[16] Fabio Ceschini G, Gatta N, Venturini M, Hubauer T, Murarasu A. Optimization of statistical methodologies for anomaly detection in gas turbine dynamic time series. Journal of Engineering for Gas Turbines and Power. 2018;**140**(3)

[17] Tsoutsanis E, Meskin N, Benammar M, Khorasani K. A dynamic prognosis scheme for flexible operation of gas turbines. Applied Energy. 2016;**164**:686-701

[18] Tsoutsanis E, Meskin N. Derivative-driven window-based regression method for gas turbine performance prognostics. Energy. 2017;**128**:302-311

[19] Stamatis A, Mathioudakis K, Papailiou KD. Adaptive simulation of gas turbine performance. Journal of Engineering for Gas Turbines and Power. 1990;**112**(2):168-175

[20] Yu Y, Chen L, Sun F, Wu C. Neural-network based analysis and prediction of a compressor's characteristic performance map. Applied Energy. 2007;**84**(1):48-55

[21] Crosa G, Pittaluga F, Trucco Martinengo A, Beltrami F, Torelli A, Traverso F. Heavy-duty gas turbine plant aerothermodynamic simulation using Simulink. In: ASME 1996 Turbo Asia Conference 1996. American Society of Mechanical Engineers Digital Collection. 1996

[22] Kim JH, Song TW, Kim TS, Ro ST. Model development and simulation of tansient behavoir of heavy duty gas turbines. Journal of Engineering for Gas Turbines and Power. 2001;**123**(3): 589-594

[23] Camporeale SM, Fortunato B, Mastrovito M. A modular code for real time dynamic simulation of gas turbines in simulink. Journal of Engineering for Gas Turbines and Power. 2006;**128**(3): 506-517

[24] Bracco S, Delfino F. A mathematical model for the dynamic simulation of low size cogeneration gas turbines within smart microgrids. Energy. 2017; **119**:710-723

[25] Fawke AJ, Saravanamuttoo HI, Holmes M. Experimental verification of a digital computer simulation method for predicting gas turbine dynamic behaviour. Proceedings of the Institution of Mechanical Engineers. 1972;**186**(1):323-329

[26] Rowen WI. Simplified mathematical representations of heavy-duty gas turbines. Journal of Engineering for Gas Turbines and Power. 1983;**105**(4): 865-869

[27] Crosa G, Ferrari G, Trucco A. Steady-state and transient performance simulation of a turboshaft engine with free power turbine. In: Proceedings of the ASME Turbo Expo. Vol. 1999. 1995

[28] MacIsaac BD, Saravanamuttoo HIH. Digital and hybrid computing techniques for simulation of gas turbine performance. In: ASME Pap: Comparison of Analog. 1974

[29] Rahman NU, Whidborne JF. A numerical investigation into the effect of engine bleed on performance of a single-spool turbojet engine. Proceedings Institution Mechanical Engineers G Journal of Aerospace Engineering. 2008;**222**(7):939-949

[30] Alexiou A, Roumeliotis I, Aretakis N, Tsalavoutas A, Mathioudakis K. Modeling contra-rotating turbomachinery components for engine performance simulations: The geared turbofan with contra-rotating core case. Journal of Engineering for Gas Turbines and Power. 2012;**134**(11)

[31] Rahman NU, Whidborne JF. Real-time transient three spool turbofan engine simulation: A hybrid approach. Journal of Engineering for Gas Turbines and Power. 2009;**131**(5)

[32] Wang C, Li YG, Yang BY. Transient performance simulation of aircraft engine integrated with fuel and control systems. Applied Thermal Engineering. 2017;**114**:1029-1037

[33] Benato A, Bracco S, Stoppato A, Mirandola A. Dynamic simulation of combined cycle power plant cycling in the electricity market. Energy Conversion and Management. 2016;**107**: 76-85

[34] Benato A, Stoppato A, Bracco S. Combined cycle power plants: A comparison between two different dynamic models to evaluate transient behaviour and residual life. Energy Conversion and Management. 2014;**87**: 1269-1280

[35] Benato A, Bracco S, Stoppato A, Mirandola A. LTE: A procedure to predict power plants dynamic behaviour and components lifetime reduction during transient operation. Applied Energy. 2016;**162**:880-891

[36] Walsh PP, Fletcher P. Gas Turbine Performance. John Wiley & Sons, Ltd; 2004

[37] MacIsaac B, Langton R. Gas Turbine Propulsion Systems. John Wiley & Sons, Ltd; 2011

[38] Rokke NA, Hustad JE, Berg S. Pollutant emissions from gas fired turbine engines in offshore practice—Measurements and scaling. ASME. International Gas Turbine and Aeroengine Congress and Exposition, GT. 1993;**1993**:1993

[39] Pires TS, Cruz ME, Colaco MJ, Alves MAC. Application of nonlinear multivariable model predictive control to transient operation of a gas turbine and NOX emissions reduction. Energy. 2018;**149**:341-353

[40] Heier S. Grid integration of wind energy: Onshore and offshore conversion systems. Grid Integration of Wind Energy. John Wiley & Sons, Ltd; 2014

[41] Alizadeh E, Meskin N, Khorasani K. A dendritic cell immune system inspired scheme for sensor fault detection and isolation of wind turbines. IEEE Transactions on Industrial Informatics. 2018;**14**(2):545-555

[42] Gao R, Gao Z. Pitch control for wind turbine systems using optimization, estimation and compensation. Renewable Energy. 2016;**91**:501-515

[43] Rezaeiha A, Kalkman I, Blocken B. Effect of pitch angle on power performance and aerodynamics of a vertical axis wind turbine. Applied Energy. 2017;**197**:132-150

[44] La Cava W, Danai K, Spector L, Fleming P, Wright A, Lackner M. Automatic identification of wind turbine models using evolutionary multiobjective optimization. Renewable Energy. 2016;**87**:892-902

[45] Tsoutsanis E, Meskin N, Benammar M, Khorasani K. Transient gas turbine performance diagnostics through nonlinear adaptation of compressor and turbine maps. Journal of Engineering for Gas Turbines and Power. 2015;**137**(9)

[46] Tsoutsanis E, Li Y, Pilidis P, Newby M. Non-linear model calibration for off-design performance prediction of gas turbines with experimental data. Aeronautical Journal. 2017;**121**(1245): 1758-1777

[47] Wan A, Gu F, Jin J, Gu X, Ji Y. Modeling and optimization of shutdown process of combined cycle gas turbine under limited residual natural gas. Applied Thermal Engineering. 2016;**101**: 337-349

[48] Buttler A, Dinkel F, Franz S, Spliethoff H. Variability of wind and solar power an assessment of the current situation in the European Union based on the year 2014. Energy. 2016;**106**: 147-161

[49] Angerer M, Kahlert S, Spliethoff H. Transient simulation and fatigue

evaluation of fast gas turbine startups and shutdowns in a combined cycle plant with an innovative thermal buffer storage. Energy. 2017;**130**: 246-257

[50] Muljadi E. Pitch-controlled variable-speed wind turbine generation. IEEE Transactions on Industry Applications. 2001;**37**(1):240-246

[51] Cheng WYY, Liu Y, Bourgeois AJ, Wu Y, Haupt SE. Short-term wind forecast of a data assimilation/weather forecasting system with wind turbine anemometer measurement assimilation. Renewable Energy. 2017;**107**:340-351